

LATTICE STRUCTURES MODELING: INTRODUCTION TO HOMOGENIZATION

¹Nikoleta Pasvanti, ¹Andreas Psarros, ²Georgios Korbetis, ³Andreas Vlahinos, ¹Athanassios Mihailidis

¹Lab. of Machine Elements & Machine Design, Aristotle University of Thessaloniki, Greece

²BETA CAE Systems S.A., Thessaloniki, Greece

³Advanced Engineering Solutions, Colorado, USA

KEYWORDS -

Lattice structures, homogenization, Schwarz's P structure

ABSTRACT -

The significance of lightweight structures is indisputable. Architected materials like complex lattice structures can nowadays be easily fabricated, due to the evolution of Additive Manufacturing (AM) technology. They contribute to reduce weight up to 80%, as well as to cost since less material is being used. Being almost as durable as a solid part, lattice structures are being more and more often used in biomechanical, automotive and aerospace applications.

A review of the conventional CAE methods revealed crucial difficulties that led to the conclusion that such approaches can be grinding and inappropriate. The purpose of this study is to propose an effective and less time-consuming modeling method via material homogenization.

Two lattice unit cells were investigated: a simple beam lattice cell with diagonal beams and the Schwarz's P cell. The appropriate load cases were run in order to calculate the stiffness matrix of the lattice cells and the results were nondimensionalized. The material behavior according to the mass fraction of the structure was investigated. Pre- and post-processing were automated by means of Python scripts. The same scripts were run to obtain the elastic properties of structures composed of more unit cells and the results obtained were evaluated.

As expected, the conventional solid mesh approach gives more accurate results but carries significant disadvantages regarding model complexity and solution time. The numerical homogenization method is effective, less time and memory consuming and allows for design freedom.

TECHNICAL PAPER –

1. INTRODUCTION

Lattice structures belong to the category of the so-called "architected" materials. They are composed of a combination of bulk material and empty space to generate a new much lighter structure, which has mechanical properties close to those of the original bulk material but less weight. They are divided into stochastic and periodic structures. Lattices form a sub - category of the latter ones, having a three – dimensional periodicity, [1].

A lattice structure is the key to produce parts which are lightweight and have good mechanical properties. Modern engineering design focuses on the concept of putting material only where it is needed and that is where lattices come in. Recent development in additive manufacturing technology make building such complex parts possible, [2].

Cost reduction due to the use of lightweight structures is significant, as the aerospace and automotive industry achieve vast fuel savings and lower emissions. The medical industry takes advantage of the lattice structures as they allow designers to emulate bio-structures.

Implementing conventional CAE tools to accurately analyze lattice structures is time and memory consuming. A huge number DOF for the finite element model and a considerable computational effort would be needed for a precise representation of the lattice structure, at the scale of the component, [3]. As the number of the individual unit cells increases, the pre – processing files become very difficult to manipulate, almost impossible to solve and the results require a considerable amount of disk space. That is why there is the need to avoid using volume mesh on the initial geometry and use an effective and less time – consuming modeling method on large and complex structures.

2. HOMOGENIZATION

From a mechanical point of view, the elementary unit cell (often referred as Representative Volume Element, “RVE”) of a lattice structure can be interpreted at the microscopic scale, as a heterogeneous medium. At the macroscopic scale, it can be modelled as an equivalent homogeneous anisotropic continuum. When dealing with the analysis and design of lattice structures, a good practice is to make use of a homogenization procedure in order to replace, at the macroscopic scale, the actual, complex geometry of the RVE by an equivalent homogeneous medium. Its mechanical response can then be described by a set of “effective” (or equivalent) material properties. Although the bulk material constituting the lattice is isotropic, its macroscopic behavior (i.e. after homogenization) can be (in the most general case) completely anisotropic because its effective elastic properties depend upon the geometrical parameters of the RVE at the lower scale, thus being affected by the RVE orientation too, [3]. In this work, orthotropic RVEs with cubic symmetry are being examined and the homogenization scheme is based on the reaction forces calculation.

The material constitutive equation of an orthotropic and linearly elastic RVE can be written as:

$$[\bar{\sigma}] = [C][\bar{\epsilon}] \quad (1)$$

where $[\bar{\epsilon}]$ is the average strain matrix, $[\bar{\sigma}]$ is the average stress matrix and $[C]$ is the stiffness matrix as shown in Eq. (2) for the orthotropic three - dimensional RVE, [4,5]:

$$\begin{bmatrix} \bar{\sigma}_{11} \\ \bar{\sigma}_{22} \\ \bar{\sigma}_{33} \\ \bar{\sigma}_{12} \\ \bar{\sigma}_{13} \\ \bar{\sigma}_{23} \end{bmatrix} = \begin{bmatrix} C_{11} & C_{12} & C_{13} & 0 & 0 & 0 \\ C_{12} & C_{22} & C_{23} & 0 & 0 & 0 \\ C_{13} & C_{23} & C_{33} & 0 & 0 & 0 \\ 0 & 0 & 0 & C_{44} & 0 & 0 \\ 0 & 0 & 0 & 0 & C_{55} & 0 \\ 0 & 0 & 0 & 0 & 0 & C_{66} \end{bmatrix} \begin{bmatrix} \bar{\epsilon}_{11} \\ \bar{\epsilon}_{22} \\ \bar{\epsilon}_{33} \\ \bar{\epsilon}_{12} \\ \bar{\epsilon}_{13} \\ \bar{\epsilon}_{23} \end{bmatrix} \quad (2)$$

For the calculation of each constant of the stiffness matrix, certain boundary conditions and displacements are imposed on the RVE in order to obtain only one component of the strain matrix different from zero. The average stress is computed by taking into account the sum of the reaction forces over the equivalent surface of the RVE. Then, the material properties can be derived from the compliance matrix $[S]$, which is the inverse of the stiffness matrix $[C]$:

$$[S] = [C]^{-1} = \begin{bmatrix} S_{11} & S_{12} & S_{13} & 0 & 0 & 0 \\ S_{12} & S_{22} & S_{23} & 0 & 0 & 0 \\ S_{13} & S_{23} & S_{33} & 0 & 0 & 0 \\ 0 & 0 & 0 & S_{44} & 0 & 0 \\ 0 & 0 & 0 & 0 & S_{55} & 0 \\ 0 & 0 & 0 & 0 & 0 & S_{66} \end{bmatrix} \quad (3)$$

The material properties are:

$$\begin{aligned} E_1 &= \frac{1}{S_{11}}, E_2 = \frac{1}{S_{22}}, E_3 = \frac{1}{S_{33}} \\ \nu_{12} &= -\frac{S_{12}}{S_{11}}, \nu_{13} = -\frac{S_{13}}{S_{11}}, \nu_{23} = -\frac{S_{23}}{S_{22}} \\ G_{12} &= \frac{1}{S_{44}}, G_{13} = \frac{1}{S_{55}}, G_{23} = \frac{1}{S_{66}} \end{aligned} \quad (4)$$

3. GEOMETRY OF LATTICE CELLS

Two different elementary unit cells were investigated: the beam lattice cell (**Fig. 1a**) and the Schwarz's P lattice cell (**Fig. 1b**). The former one was chosen due to the simplicity of the structure and the manageability of the model. The latter one features a completely different geometry from the first, as it is based on the Schwarz's P ("Primitive") minimal surface. These lattices can be easily built by additive manufacturing.

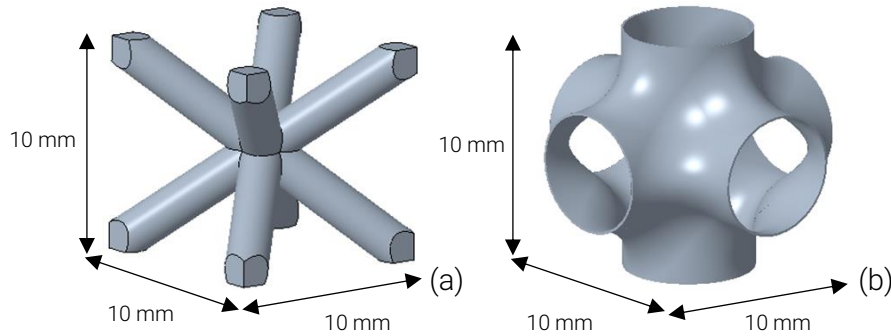


Fig. 1. Unit lattice cells. (a) Beam lattice cell; (b) Schwarz's P cell

Both the geometries have outer dimensions 10 mm x 10 mm x 10 mm. The geometric parameter used for the beam unit cell is the mass fraction (m.f.), which is controlled by the diameter d of the beams, **Fig. 2**. The same geometric parameter was used for the Schwarz's P cell as well. It was changed by altering the thickness t of the cell, **Fig. 3**.

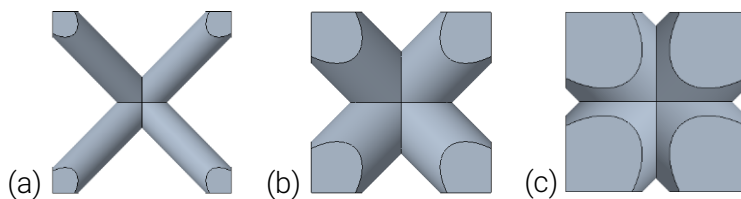


Fig. 2. Beam unit cell.
(a) $d=2$ mm, m.f.=18%
(b) $d=4$ mm, m.f.=56%
(c) $d=6$ mm, m.f.=90%

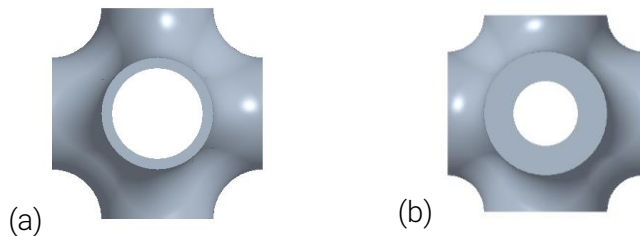


Fig. 3. Schwarz's P unit cell.
(a) $t=0,5$ mm, m.f.=12%
(b) $t=1,5$ mm, m.f.=35%

4. WORKFLOW AND FE METHOD

At first, two modelling parameters were examined aiming at choosing the most appropriate ones: the finite element length and the element type.

The procedure followed is the one mentioned below:

- Input of the CAD geometry in ANSA
- Automated pre – processing of the model using a Python script. The same uniform mesh was generated in each beam to avoid mesh discrepancy effects on the results. The appropriate boundary and loading conditions were also imposed through the script. Due to the orthotropic material and the cubic symmetry, the elastic properties remain the same towards every direction (Eq. 5). Thus, two runs were required. The first one applied for the calculation of E_{eff} and ν_{eff} with the boundary conditions depicted in **Fig. 4** and the second one for the calculation of G_{eff} (**Fig. 5**)

$$E_1 = E_2 = E_3 = E ; \nu_{12} = \nu_{23} = \nu_{13} = \nu ; G_1 = G_2 = G_3 = G \quad (5)$$

- Output of the model and solution in ABAQUS
- Results input into META post – processor
- Effective material properties calculation (E_{eff} , ν_{eff} , G_{eff}) through an automated script in Python programming language

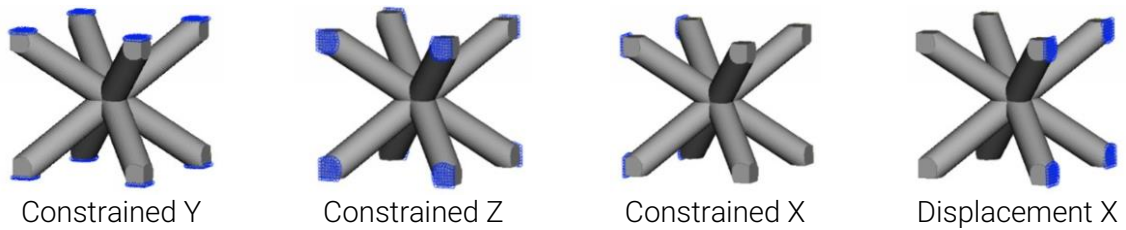


Fig. 4. Constraints applied to calculate E_{eff} and ν_{eff}

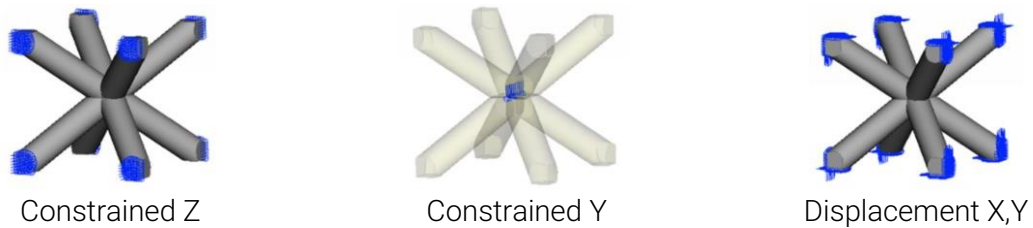


Fig. 5. Constraints applied to calculate G_{eff}

5. RESULTS

5.1. FE Modeling

5.1.1. Beam Lattice Cell

C3D4 Elements: Starting with the beam lattice cell and using the ABAQUS C3D4 elements (first order, tetrahedral elements), the effect of the FE length is investigated. The parameter of fillet radius is also introduced, as no such structure is feasible to be built without a fillet radius. (Fig. 6) The unit cell with $R = 0$ and the unit cell with $R = 1$ mm have a volume difference of only 2%.

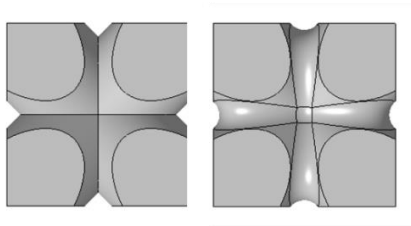


Fig. 6. Beam lattice unit cell without (left) and with fillet radius (right)

The following Fig. 7, 8 and 9 show the convergence of the elastic properties' values when computed using the above mentioned first order elements. Selecting a FE length of 0,1 mm results in good accuracy and the following number of elements: 455264, 1260736 and 1752000 elements for the structures with beam diameters 2, 4 and 6 mm respectively.

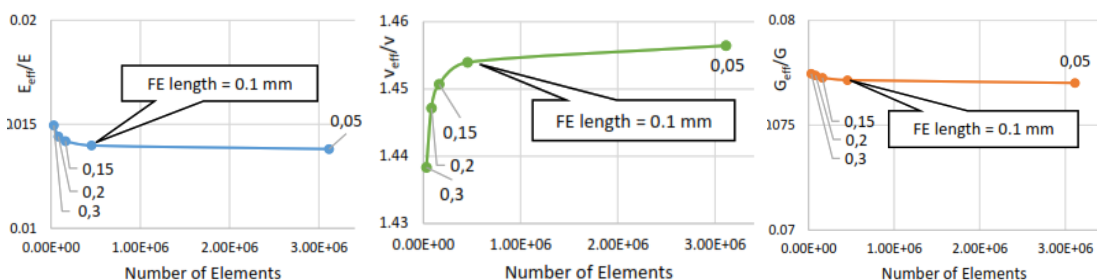


Fig. 7. Material properties ratio over number of C3D4 elements for $d = 2$ mm (m.f.=18%)

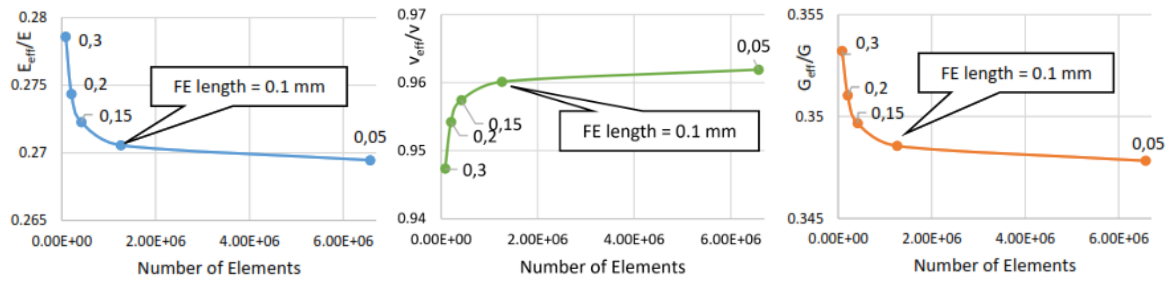


Fig. 8. Material properties ratio over number of C3D4 elements for d = 4 mm (m.f.=56%)

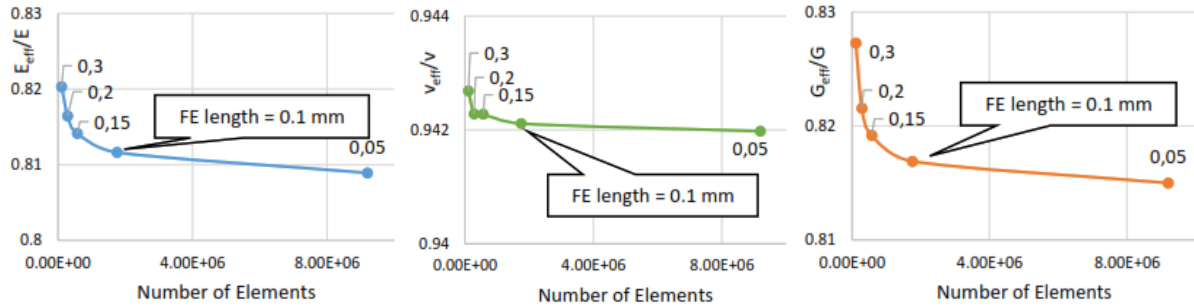


Fig. 9. Material properties ratio over number of C3D4 elements for d = 6 mm (m.f.=90%)

C3D10 Elements: Further investigation introduced the 2nd order tetrahedral ABAQUS C3D10 elements. The same accuracy as with the 1st order elements could be achieved with greater element length (0,5 mm) and consequently, a significant reduction in the number of elements and CPU time needed, as it can be clearly seen in Fig. 10, 11 and 12. Specifically, for the structure with the beam diameter d = 2 mm, 7536 elements were needed, whereas for the diameters d = 4 mm and d = 6 mm, the number of elements was 20152 and 29208 respectively.

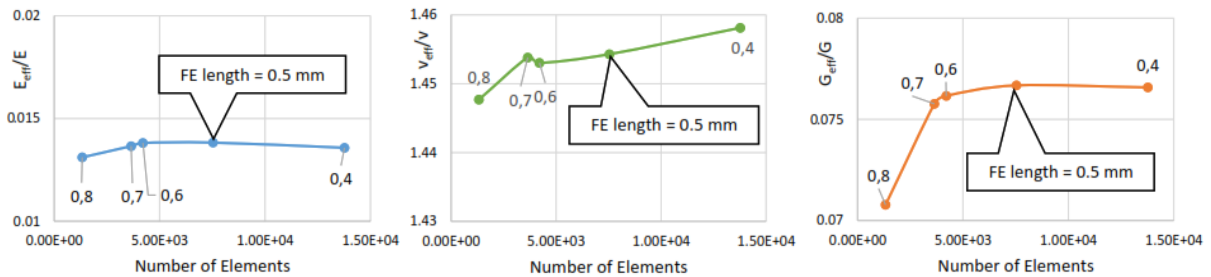


Fig. 10. Material properties ratio over number of C3D10 elements for d = 2 mm (m.f.=18%)

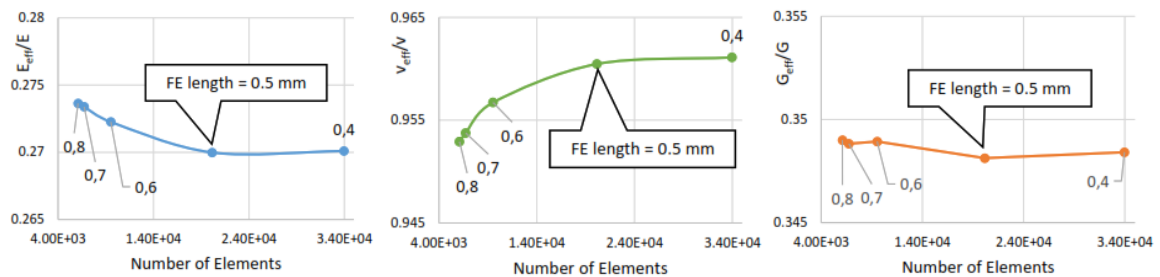


Fig. 11. Material properties ratio over number of C3D10 elements for d = 4 mm (m.f.=56%)

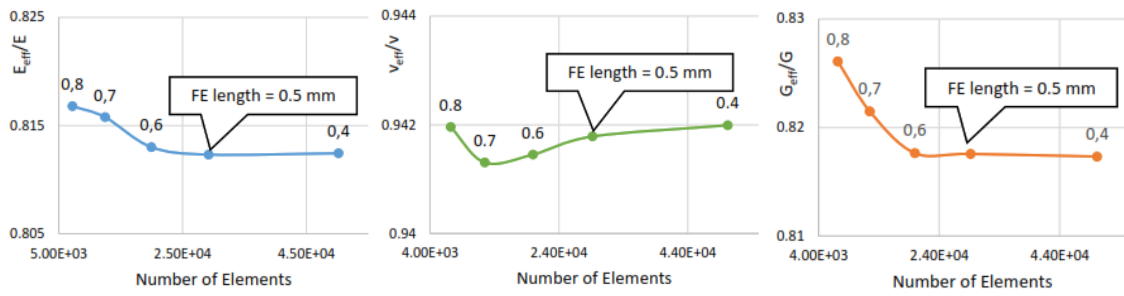


Fig. 12. Material properties ratio over number of C3D10 elements for $d = 6$ mm (m.f.=90%)

Table 1 shows the improvement in CPU time achieved when using 2nd order C3D10 elements instead of C3D4 ones.

Table 1. Comparison of 1st and 2nd order elements concerning CPU time. The accuracy is the same

	Element type	C3D4 (1 st order)	C3D10 (2 nd order)	Ratio
d=2, m.f.=18%	Time [s]	1048	40	26,53 : 1
	Nodes	84707	13185	6,42 : 1
d=4, m.f.=56%	Time [s]	3877	266	14,58 : 1
	Nodes	241361	31845	7,58 : 1
d=6, m.f.=90%	Time [s]	6590	171	38,63 : 1
	Nodes	323745	43961	7,36 : 1

5.1.2. Schwartz's P Lattice Cell

Based on the experience gained with the beam element, the material properties of the Schwarz's P unit cell were calculated using C3D10 elements. The results obtained for two unit cells with mass fractions 12% (wall thickness 0,5 mm) and 35% (wall thickness 1,5 mm) are shown in Fig. 13 and 14. Sufficient convergence could be achieved at a FE length of 0,3 mm for both structures. The corresponding number of elements was 30360 elements for the thin structure and 54704 elements for the thick one.

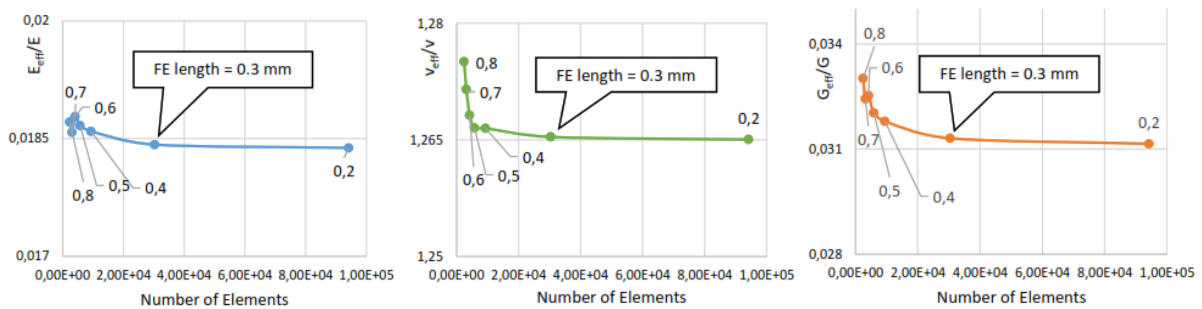


Fig. 13. Material properties ratio over number of C3D10 elements for $t = 0,5$ mm (m.f.=12%)

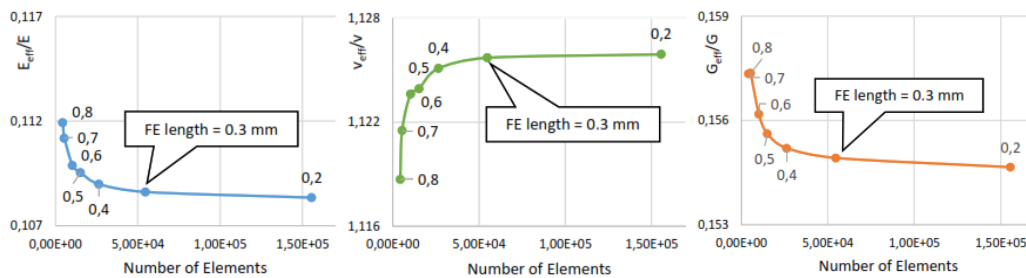


Fig. 14. Material properties ratio over number of C3D10 elements for $t = 1,5$ mm (m.f.=34%)

5.2. Verification

A first indication that the results are qualitatively correct, is the fact that computed E_{eff} , ν_{eff} and G_{eff} of the lattice cell tend to the values of the bulk material as the mass fraction increases.

However, in order to take into account, the “free edge effect” and increase the accuracy, lattice structures composed of multiple cells have to be analyzed. In the current study, a 3x3x3 (Fig.15a) and a 6x6x6 beam lattice structure (Fig.15b) was modelled using C3D10 type elements and FE length = 0,5 mm, as well as well as a 3x3x3 Schwarz’s P structure (Fig. 16) with wall thickness = 1,5 mm, C3D10 elements and FE length = 0,3 mm. The results and the deviations are depicted in Table 2 and 3. It can be clearly concluded that, the accuracy obtained with 3x3x3 structures is very good.

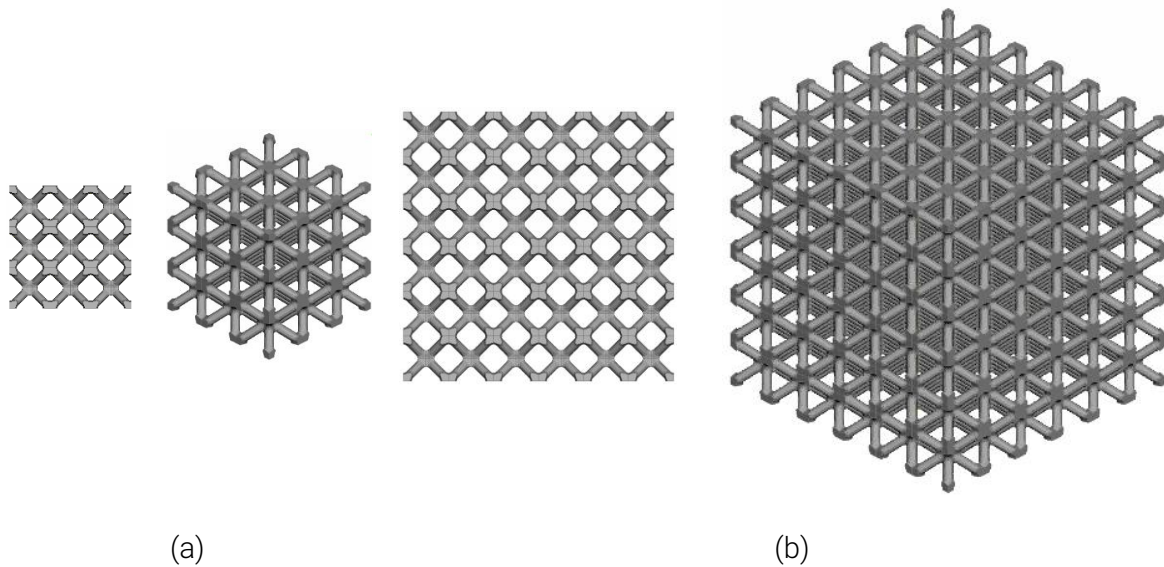


Fig. 15. Beam lattice structure with (a) 3x3x3 units and (b) 6x6x6 unit cells

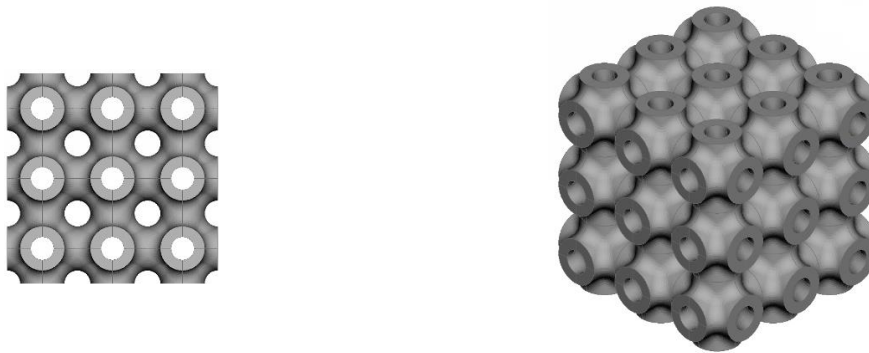


Fig. 16. 3. Schwarz’s P lattice structure with 3x3x3 unit cells

Table 2: Convergence of the calculated properties when increasing the count of unit cells

Beam Lattice, d=2 , m.f.=18%	1x1x1	3x3x3	Deviation	6x6x6	Deviation
E_{eff}	2903,78	2866,28	-1,31%	2865,96	-0,01%
G_{eff}	6210,94	6297,96	1,38%	6325,27	0,43%
ν_{eff}	0,436	0,437	0,13%	0,437	0,00%

Table 3: Convergence of the calculated properties when increasing the count of unit cells

Schwarz's P Lattice, $t=1,5$ mm, $m.f.=35\%$	1x1x1	3x3x3	Deviation
E_{eff}	22807,23	22807,29	0,00%
G_{eff}	12548,41	13774,46	8,90%
V_{eff}	0,338	0,338	0,00%

6. CONCLUSIONS

Actual parts featuring lattices are almost impossible to model and solve by simply meshing the initial geometry using solid mesh. For instance, a simple beam lattice of a diameter of 2 mm with 12 cells in each direction requires about 15 million elements to provide trustworthy results. That is why material homogenization becomes essential.

In order to get precise material properties, a correct choice of the type of elements and the FE length must be made. According to the two types of unit cells investigated, 2nd order elements, like the ABAQUS C3D10 ones, provide accurate results with the acceptable cost in solution time once the element length is chosen properly to match cell geometry.

As the number of the unit cells in each direction increases, the material properties converge to certain values. According to this study, a lattice of 6x6x6 unit cells provides a very good approximation to the actual properties of the lattice.

REFERENCES

- (1) Abdul Hadi Azman. Method for integration of lattice structures in design for additive manufacturing. Materials. Université Grenoble Alpes, 2017. English.
 - (2) W. Tao, M. C. Leu, Design of lattice structures for additive manufacturing. 2016 Int. Symp. Flex. Autom., 1–3 (2016).
 - (3) Giorgio De Pasqualea, Marco Montemurro, Anita Catapanoc, Giulia Bertolino and Luca Revellia. 2018. Cellular structures from additive processes: design, homogenization and experimental validation. Procedia Structural Integrity 8: 75 – 82
 - (4) Fan Ye and Hu Wang. 2017. A simple Python code for computing effective properties of 2D and 3D representative volume element under periodic boundary conditions. arXiv:1703.03930
 - (5) Kelly, P. 2013. Solid mechanics part I: An introduction to solid mechanics. Solid mechanics lecture notes, University of Auckland. pp. 156 – 166.
-